

PERSPECTIVE | NOVEMBER 01 2024

Probing photochemical dynamics using electronic vs vibrational sum-frequency spectroscopy: The case of the hydrated electron at the water/air interface

Special Collection: [Festschrift in honor of Yuen-Ron Shen](#)

Faith G. Pritchard ; Caleb J. C. Jordan ; Jan R. R. Verlet  



J. Chem. Phys. 161, 170901 (2024)

<https://doi.org/10.1063/5.0235875>



View
Online



Export
Citation

Articles You May Be Interested In

Development of phase-cycling interface-specific two-dimensional electronic sum frequency generation (2D-ESFG) spectroscopy

J. Chem. Phys. (September 2024)

Time-resolved heterodyne-detected electronic sum frequency generation (TR-HD-ESFG) spectroscopy: A new approach to explore interfacial dynamics

J. Chem. Phys. (November 2024)

Femtosecond time-resolved electronic sum-frequency generation spectroscopy: A new method to investigate ultrafast dynamics at liquid interfaces

J. Chem. Phys. (March 2008)

20 November 2024 08:53:01



The Journal of Chemical Physics

Special Topics Open for Submissions

[Learn More](#)

Probing photochemical dynamics using electronic vs vibrational sum-frequency spectroscopy: The case of the hydrated electron at the water/air interface

Cite as: J. Chem. Phys. 161, 170901 (2024); doi: 10.1063/5.0235875

Submitted: 30 August 2024 • Accepted: 15 October 2024 •

Published Online: 1 November 2024





View Online



Export Citation



CrossMark

Faith G. Pritchard,  Caleb J. C. Jordan,  and Jan R. R. Verlet^{a)} 

AFFILIATIONS

Department of Chemistry, Durham University, Durham DH1 3LE, United Kingdom

Note: This paper is part of the JCP Festschrift in Honor of Yuen-Ron Shen.

^{a)} Author to whom correspondence should be addressed: j.r.verlet@durham.ac.uk

ABSTRACT

Photo-dynamics can proceed differently at the water/air interface compared to in the respective bulk phases. Second-order non-linear spectroscopy is capable of selectively probing the dynamics of species in such an environment. However, certain conclusions drawn from vibrational and electronic sum-frequency generation spectroscopies do not agree as is the case for the formation and structure of hydrated electrons at the interface. This Perspective aims to highlight these apparent discrepancies, how they can be reconciled, suggests how the two techniques complement one another, and outline the value of performing both techniques on the same system.

© 2024 Author(s). All article content, except where otherwise noted, is licensed under a Creative Commons Attribution (CC BY) license (<https://creativecommons.org/licenses/by/4.0/>). <https://doi.org/10.1063/5.0235875>

INTRODUCTION

The aqueous/air interface is one of the most abundant interfaces on Earth with two-thirds of the surface covered by ocean waves, sprays, and aerosols; with fogs, clouds, and atmospheric water; and with snowpacks and polar regions. Consequently, understanding the chemical and physical processes at the water/air interface is one of the major contemporary scientific challenges. The water/air interface is particularly important from an atmospheric chemistry perspective, and experimental evidence indicates that reactions can be accelerated or unexpected reactivity can be induced compared to bulk aqueous reactions.^{1–7} These differences arise because of the unique environment at the interface that is unlike either of the adjoining bulk phases (water or air/vacuum), where there exist large density gradients, differing concentrations of solutes, alignment and orientational effects, and strong electric fields.^{8,9} Photochemistry, in particular, is expected to be affected by interfacial effects as excited states are often more sensitive to perturbations, on account of the weaker electron binding, such that their potential energy surfaces and internal conversion pathways might be expected to differ from those in either bulk phases.^{6,10–12} Take the case of the protonated

tryptophan S_1 excited state, which decays by ultrafast internal conversion in the gas-phase, but the addition of just two water molecules leads to a much slower decay (as observed in bulk water),¹³ or the deprotonated green fluorescent protein chromophore anion for which the addition of two water molecules shifts the $S_1 \leftarrow S_0$ absorption maximum by 1000 cm^{-1} .¹⁴ While these examples highlight the sensitivity to microhydration, they are not representative of a macroscopic water/air interface.

To probe molecules at the interface between two phases, whose signatures would otherwise be lost among those from the bulk, second- (or even-) order non-linear spectroscopy has been developed by Shen and others.^{15–23} The basic premise is that only in non-centrosymmetric media will elements of the second-order non-linear electric susceptibility tensor be non-zero, $\chi^{(2)} \neq 0$.²⁴ At the water/air interface, bulk water and air are centrosymmetric, but the interface between the two is—by definition—not so that the polarization induced at the water/air interface (or indeed any interface with differing refractive indices) will produce a second-order response, leading to second-harmonic generation (SHG) or sum-frequency generation (SFG). The simplest experiment involves the detection of photons of frequency ω_{SFG} generated by the coherent

addition of two photons of ω_1 and ω_2 , where $\omega_{\text{SFG}} = \omega_1 + \omega_2$ or $\omega_{\text{SHG}} = 2\omega$. The homodyne-detected intensity of $\omega_{\text{SF/HG}}$, $I_{\text{SF/HG}}$, is proportional to $|\chi^{(2)}|^2$ and may be enhanced when any of the fields $\omega_{\text{SF/HG}}$, ω_1 , or ω_2 are resonant with some transition of the medium, thus allowing for the detection of specific resonances, or species, at an interface and the study of their dynamics.

As $\chi^{(2)}$ is a complex tensor, homodyne-detected SFG is inherently limited, and ideally, one would aim to measure the imaginary component of $\chi^{(2)}$, $\text{Im}(\chi^{(2)})$, which is proportional to the concentration of (resonant) species at the interface. This can be done through interference or heterodyne-detected (HD) SF/HG, where the surface nonlinear signal is temporally or spectrally interfered with a local oscillator field.²⁵ The development of HD-SFG,²⁶ in particular, has led to a number of exciting advancements in the field.^{22,27–35}

Even in the early development of non-linear spectroscopy as a probe of the water/air interface, interest turned to its use in elucidating chemical photo-dynamics. For example, time-resolved electronic SHG, TR-ESHG, was used to demonstrate how the aqueous interfacial environment slows the excited state isomerization of bulky organic dye molecules,³⁶ how intermolecular energy transfer between a donor and acceptor molecule is accelerated because of the reduced dimensionality,³⁷ and how rotational dynamics are impacted by the water/air surface.³⁸ While several experiments have employed TR-ESFG since to probe various dynamical processes at the interface,^{39–47} over the past decades, the focus has drifted toward vibrational SFG, VSFG. One reason for this is the bandwidth of commercial femtosecond lasers suffices to cover a relatively wide vibrational spectral range in a single shot, removing the need for tuning. For the water/air interface, the most common region of spectral interest is the OH stretch, which is typically accessed through SFG of the spectrally narrowed 800 nm output from a Ti:Sapphire laser and the output of a broad-band optical parametric amplifier in the OH stretching region ($\sim 3000\text{--}3800\text{ cm}^{-1}$), resulting in SFG light around 630 nm, which can be readily measured using silicon detectors. Extension to HD-VSFG and even time-resolved (TR) HD-VSFG is no longer uncommon although the experimental arrangements are nontrivial.²³ The application of these methods has offered a remarkable insight into the nature of the neat water/air interface.^{48–50}

(HD-)VSFG methods applied to probe species adsorbed at the water/air interface offer either direct information about vibrational spectra of adsorbates or about changes in solvating water molecules in response to the adsorbate. In terms of photochemistry at the water/air interface, the latter has often been applied. Specifically, changes in the water OH stretch offer a probe of new species being formed following photoexcitation as water interacts with these new species. A most striking example of such an application was the photochemistry following phenol excitation, where the rate of photo-oxidation was observed to increase by a factor or 10^4 at the water/air interface compared to either flanking bulk phases.⁶ However, one could critically argue that probing the OH stretch response to phenol excitation is a rather indirect probe, affected by phenol's excited states and the other products formed (phenoxyl radical, PhO^\bullet , hydrated electron, $e_{(\text{aq})}^-$, and hydronium cation, H_3O^+). A more direct probe would be to use the optical spectra of the species produced, either vibrational or electronic. The former would be complicated because of overlapping features

(especially for $e_{(\text{aq})}^-$ and H_3O^+), whereas the latter offers a more direct probe as $e_{(\text{aq})}^-$ has a well-known and distinctive spectrum^{51,52} in the visible where features are less spectrally congested. However, time-resolved electronic SFG, TR-ESFG, presents significant (but surmountable) technical challenges: electronic spectra are typically broad so that ESFG requires very large bandwidths,^{47,53} HD-ESFG is more demanding because the shorter wavelengths require better phase stability,⁵⁴ and photoexcitation often leads to fluorescence that can easily overwhelm the very weak SFG response.⁵⁵

While TR-ESFG and TR-VSFG can probe the same photochemical process, the interpretation of their results can lead to differing conclusions. The aim of this Perspective is to highlight discrepancies between TR-VSFG vs TR-ESFG interpretations, with a focus on the formation of $e_{(\text{aq})}^-$ and the excited state dynamics of phenol and phenolate, to provide some possible explanations for these discrepancies, and to offer an outlook of future directions.

SIGNATURE OF THE HYDRATED ELECTRON IN ELECTRONIC AND VIBRATIONAL SFG SPECTROSCOPIES

As one of the most fundamental solutes in chemistry, $e_{(\text{aq})}^-$ plays a critical role in understanding quantum solvation, and it has importance in, for example, water remediation, radiation chemistry, plasma science, and nuclear chemistry.^{52,56,57} The most characteristic spectral signature of the hydrated electron is its strong and broad electronic absorption spectrum, peaking at 720 nm in bulk water, as shown in Fig. 1(a).⁵¹ The absorption arises from the nominally s-like ground electronic state of $e_{(\text{aq})}^-$ to the first excited p-states [inset Fig. 1(a)].⁵² The absorption spectrum extends far into the blue, associated with excitation to higher-lying, bound but diffuse energy levels.⁵⁸

While being a simple system in principle, $e_{(\text{aq})}^-$ has generated many decades of debate about its structure,^{52,62–66} excited state dynamics,^{67–69} and solvation at aqueous interfaces.^{7,70–73} There is a consensus that the electron resides in a roughly spherical cavity so that the $p \leftarrow s$ transition can be thought of as an excitation between the ground and excited states of a particle in a roughly spherical (finite) box.⁵² It is also generally accepted that the excited p-states are very short lived (~ 50 fs) and that subsequent relaxation predominantly involves thermalization dynamics.^{60,68,69} However, what has been more difficult to assert has been the dynamics of $e_{(\text{aq})}^-$ at an ambient water/air interface, in part, because of the limited array of surface specific probes and the low number densities of interfacial species. Nevertheless, much insight about $e_{(\text{aq})}^-$ at interfaces can be gleaned from gas-phase molecular clusters, $(\text{H}_2\text{O})_n^-$, where most water molecules reside at the water/vacuum interface.^{52,74–77} For example, experimental work has included IR (action),^{61,76,78,79} electronic (action),^{80,81} and photoelectron spectroscopy^{75,77,82–84} over a range of cluster sizes, n . A representative IR spectrum in the OH-stretching region is shown in Fig. 1(b) for $(\text{H}_2\text{O})_6^-$.^{61,76} In clusters, the excess electron can reside either external to the cluster, $e_{(\text{ext})}^-$, which is the dominant isomer observed for smaller cluster $(\text{H}_2\text{O})_{n<11}^-$, and/or submerged in the interface, $e_{(\text{surf})}^-$, which is dominant for larger clusters [representative isomers are shown in Fig. 1(c)].^{52,59} The spatial extent of the $e_{(\text{ext})}^-$ wavefunction is much larger than that of $e_{(\text{surf})}^-$, which is similar to $e_{(\text{aq})}^-$ [Fig. 1(c)].^{52,66}

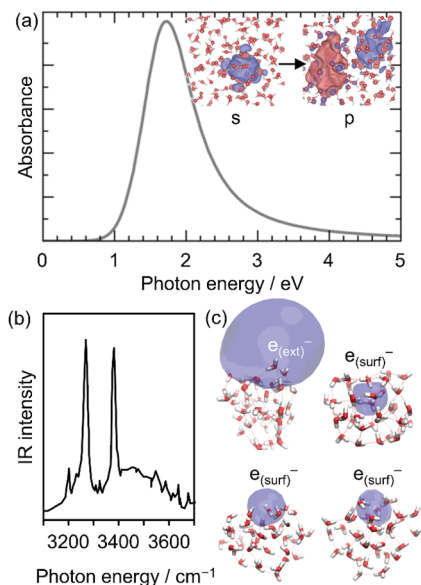


FIG. 1. (a) Electronic absorption spectrum of the hydrated electron involving the ground electronic s-state being excited to the first excited p-state(s), the orbitals of which are shown in the inset. (b) IR (action) spectrum of the $(\text{H}_2\text{O})_6^-$ cluster in the OH stretching region, where the doublet is associated with a single water molecule pointing both its H-atoms toward the electron density. (c) Structures of water cluster anions in which the electron is bound in differing solvation states, including the externally solvated electron, $e_{(\text{ext})}^-$, surface and interfacial solvated electron, $e_{(\text{surf})}^-$, which is located near the interface but has the radial distribution function similar to that of the fully hydrated electron, $e_{(\text{aq})}^-$ (and it is labeled as such in Ref. 69). (a) Inset adapted with permission from Low *et al.*, Nat. Commun. **13**(1), 7300 (2022). Copyright 2022 Springer Nature Limited. (b) Adapted with permission from Hammer *et al.*, J. Chem. Phys. **123**(24), 244311 (2005). Copyright 2005 AIP Publishing LLC. (c) Adapted with permission from Elkins *et al.*, Science **342**(6165), 1496–1499 (2013). Copyright 2013 American Association for the Advancement of Science.

Correspondingly, the binding energy of $e_{(\text{ext})}^-$ is lower than that of $e_{(\text{surf})}^-$ and $e_{(\text{aq})}^-$, implying a higher reactivity of $e_{(\text{ext})}^-$.^{70,85} However, how these cluster studies relate to a macroscopic or ambient water/air interface has been difficult to determine.

In the context of an ambient water/air interface and its relation to the structures shown in Fig. 1(c), here we refer to the $e_{(\text{ext})}^-$ form as one where most of the electron density is protruding out of the aqueous phase and into the vapor phase. On the other hand, $e_{(\text{surf})}^-$ has most of its electron density in the liquid, rather than the vapor phase, and has a spatial distribution similar to that of the bulk hydrated electron. Finally, $e_{(\text{aq})}^-$ is the fully hydrated electron that resides some way below the dividing surface in a centrosymmetric bulk environment and should not be observable using non-linear spectroscopy (which is not accurately represented by clusters as these are too small).

In principle, one might anticipate a strong surface affinity for $e_{(\text{aq})}^-$, given it is structure-breaking and has a very large polarizability, which similarly drives atomic anions, such as iodide, to the water/air interface.⁸⁶ Computationally, the main observations have been that the electron, over time, prefers to be internally solvated: for a diffuse electron initially formed at the air (vacuum) side, $e_{(\text{ext})}^-$ evolves on a ~ 1 ps timescale to a more compact $e_{(\text{surf})}^-$. Beyond

this, $e_{(\text{surf})}^-$ then evolves into $e_{(\text{aq})}^-$ on a ~ 10 ps timescale.⁸⁷ Experimentally, however, probing the electron at the interface has been challenging. While photoelectron spectroscopy on liquid microjets has provided some insight, the surface sensitivity of these methods remains ambiguous.^{70,88} Similarly, cluster studies are not directly comparable to bulk liquid structures as the clusters are cryogenic and, therefore, closer to a solid phase (ice) than liquid water. Nevertheless, some of the data of clusters can be extrapolated accurately to the bulk,⁶⁸ including the evolution of $e_{(\text{ext})}^-$ to $e_{(\text{surf})}^-$ on a ~ 1 ps timescale.⁸⁹ Second-order non-linear spectroscopy would appear to be the ideal probe.

Both TR-ESFG and TR-VSFG have been used to explore the nature of $e_{(\text{aq})}^-$ and whether it appears more like $e_{(\text{ext})}^-$ or $e_{(\text{surf})}^-$.^{7,72,73,90} Methods have generally relied on the photodetachment of an interfacial species to generate the electron locally. For ESFG, iodide was used.^{72,90} Early experiments used TR-ESHG (where the SHG was resonance enhanced with the $p \leftarrow s$ transition) of a 2M NaI solution excited at 250 nm to drive the charge-transfer-to-solvent (CTTS) transition.⁷² These experiments showed dynamics similar to those observed by transient absorption in the bulk,^{91–93} following the production and decay of $e_{(\text{aq})}^-$. A more detailed experiment probing the same CTTS process used a phase-sensitive TR-ESHG approach, where changes in phase can be correlated with changes in resonance-enhancement.⁹⁴ A selection of the results is shown in Figs. 2(a) and 2(b) for differing allowed polarization combinations (denoted PP and Smix, which refer to the polarizations of the SHG and fundamental fields relative to the surface, respectively), where ω was at a wavelength of 1320 nm (so that ω_{SHG} was at 660 nm). The PS polarization combination is broadly similar to that of the PP, and dynamics with ω at 800 nm were qualitatively similar to those presented in Fig. 2.⁹⁴ A schematic of the evolution from the CTTS state to hydrated in terms of potential energy curves along with resonant transitions is shown in Fig. 2(c).

The observed dynamics are broadly consistent (although faster) with those observed in bulk water, where the CTTS evolves into a contact pair of the iodine and electron, which cools within the first few picoseconds.^{91–93} The most striking observation, however, is the rapid change in phase in the Smix polarization combination, which is not observed in PP or PS, and the faster kinetics in this polarization combination (~ 200 fs for Smix compared to ~ 500 – 700 fs for PP and PS). A very short lifetime has previously been seen in fluorescence up-conversion experiments of the initially excited CTTS state,⁹⁵ suggesting that the Smix polarization combination is sensitive to the CTTS state at early times [i.e., the downward transition which the SHG is resonant with, Fig. 2(c)]. A non-adiabatic transition from CTTS forms the hot $e_{(\text{aq})}^-$ in a contact pair with iodine. The fundamental probe wavelength is also resonant with the electron in the contact pair, and the ultrafast $\sim \pi/2$ phase-shift appears to be a signature of the nonadiabatic transition (as it evolves from “emission” to “absorption”). The PP and PS combinations are not sensitive to the CTTS if its transition moment lies parallel to the surface (S-polarization) and only ω_{SHG} is resonantly enhanced. In the contact pair, $e_{(\text{surf})}^-$ is roughly spherical and all polarizations (Smix, PP, and PS) are sensitive to the contact pair, as shown schematically in Fig. 2(d).⁹⁰ While the detailed insight gained in the sub-picosecond dynamics following photo-oxidation of iodide at the water/air interface is remarkable, the conclusion is that the contact pair formed, which contains $e_{(\text{surf})}^-$, is broadly similar at the

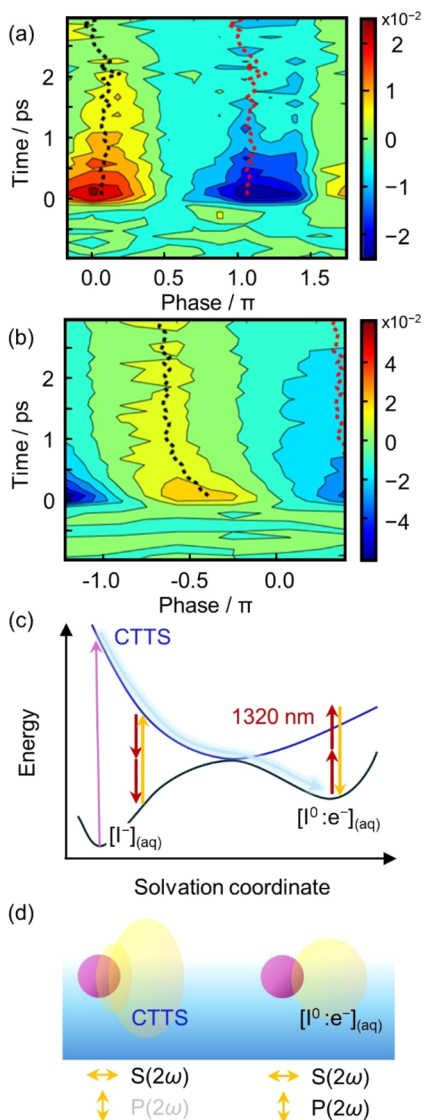


FIG. 2. Transient SHG signal as a function of phase following charge-transfer-to-solvent excitation of iodide at the water–air interface, probed with a 1320 nm probe, (660 nm), with polarization combinations (a) PP and (b) Smix. (c) Energy-level diagram of excited state processes at the water/air interface. (d) Schematic diagram of electronic distributions associated with the photooxidation of iodide, showing that the S-polarized SHG field is sensitive to the CTTS, which has a transition moment parallel to the interface, whereas the contact pair and the species separately solvated are roughly spherical and sensitive to both SHG polarizations. Adapted with permission from Nowakowski *et al.*, *J. Phys. Chem. Lett.* 7(20), 4079–4085 (2016). Copyright 2016 American Chemical Society.

interface as in bulk water. However, at 2M NaI, symmetry is broken over an extended region of the interface⁸⁶ so that the surface sensitivity in these experiments is likely limited, which may explain why the longer-time dynamics associated with geminate recombination and contact-pair dissociation are similar to those observed in the bulk. Additionally, the electron was formed in a contact pair, which may

not be representative of a “free” hydrated electron, and at very high concentrations, hydrated dielectrons may also form.⁹⁶

The formation of $e_{(aq)}^-$ has also been probed using TR-HD-VSFG experiments by Tahara and co-workers.⁷³ The formation and decay of different species at the water/air interface can be followed using their influence on the surrounding water molecules by measuring the change in the $\text{Im}(\chi^{(2)})$ signal associated with water OH stretches following the (photoinduced) generation of a new species. Two-photon ionization of water produces OH^\bullet , $e_{(aq)}^-$, and H_3O^+ : at the water/air interface, a positive $\text{Im}(\chi^{(2)})$ signal centered around 3260 cm^{-1} was observed, which decays non-exponentially on a ps time scale (with the fastest component being 0.4 ps), as shown in Fig. 3(a).⁷³ The $\text{Im}(\chi^{(2)})$ spectrum of H_3O^+ is known at the water/air interface⁹⁷ and is inconsistent with the observed spectrum, leaving either the electron or OH^\bullet as possible products. To discount the latter, photo-detachment of indole following excitation to its S_1 state was also performed.⁷³ A global fitting procedure (singular value decomposition) on the time-resolved $\text{Im}(\chi^{(2)})$ spectra was required and offered two spectral features: one decaying non-exponentially on a ps timescale [with the fastest component being 1.2 ps, Fig. 3(b)] and a second feature that hardly decayed over 300 ps [Fig. 3(c)]. They assigned the latter to water interacting with the indole cation, while the former, which peaks at 3430 cm^{-1} , has a similar overall shape to the spectrum in Fig. 3(a). Both the features in Figs. 3(a) and 3(b) were assigned to the electron at the water/air interface. The blue-shift of 170 cm^{-1} exhibited in Fig. 3(b) was accounted for by the interaction of the electron with the indole cation.⁷³ The two features associated with the hydrated electron also exhibit a small, slower decay component with lifetimes of 22 and 57 ps [see Figs. 3(a) and 3(b), respectively]. The authors also correlated the $\text{Im}(\chi^{(2)})$ spectrum with IR (action) spectra from water cluster anions [see Fig. 2(a)]⁶¹ and argued that the similar general shape was an indication that the binding of the electron at the water/air interface is similar to that of small clusters,⁷⁶ i.e., $e_{(ext)}^-$ [see Fig. 1(c)].

The conclusion from the TR-HD-VSFG experiments appears to be at odds with those from TR-ESHG: the former proposes an electron that appears to be more akin to $e_{(ext)}^-$, while the latter appears to be more akin to $e_{(surf)}^-$. However, one can argue that the electron sources were also very different: the parent species may be solvated at different depths with respect to the dividing surface,⁷³ and their steric and electrostatic character may affect the chemical environment into which the electron is ejected. Recently, two studies have reported on the photochemistry of phenolate⁷ and phenol⁶ at the water/air interface, which offers a closer comparison (albeit not perfect either). These are considered in the sections titled “Excited state dynamics of phenolate and the electronic signature of the hydrated electron” and “Excited state dynamics of phenol and enhanced photo-chemical reactivity.”

EXCITED STATE DYNAMICS OF PHENOLATE AND THE ELECTRONIC SIGNATURE OF THE HYDRATED ELECTRON

Jordan *et al.* studied the electron ejection from phenolate following excitation to its S_1/S_2 excited state (at 257 nm) using TR-ESFG.^{7,12} The observed kinetics are similar to those observed in the bulk using transient absorption spectroscopy^{98–100} but about

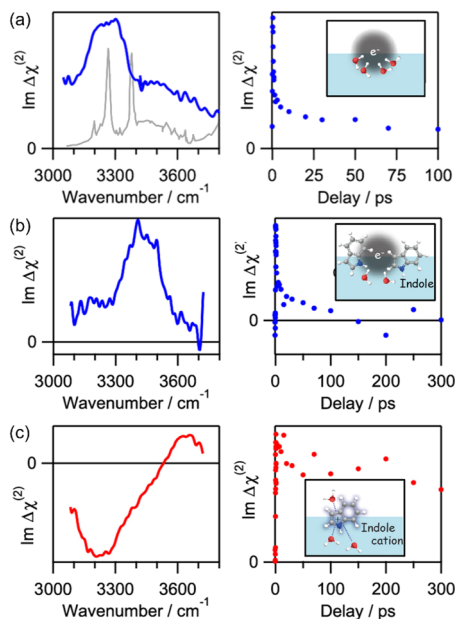


FIG. 3. Vibrational $\text{Im}(\chi^{(2)})$ spectra (blue/red lines) and kinetics (blue/red circles) associated with OH stretch of water at the water/air interface for a hydrated electron formed by two-photon excitation of water (a), the hydrated electron formed by photo-oxidation of indole (b), and the indole cation remaining following the latter photo-oxidation (c). Schematics of the electron distribution at the water/air interface are shown in the inset. The gray spectrum in (a) is the IR action spectrum for $(\text{H}_2\text{O})_6^-$ from Fig. 1(b). Adapted with permission from Matsuzaki *et al.*, *J. Am. Chem. Soc.* **138**(24), 7551–7557 (2016). Copyright 2016 American Chemical Society.

2–3 times faster at the interface.¹² However, longer-time dynamics appeared somewhat different, with a slow decay tentatively assigned to loss of the electron from the surface: $e_{(\text{surf})}^- \rightarrow e_{(\text{aq})}^-$.¹² This was subsequently confirmed in a scanning TR-ESFG experiment, where one of the driving fields, ω_1 , was tuned over the broad $p \leftarrow s$ resonance of $e_{(\text{aq})}^-$ [Fig. 1(a)], which simultaneously also led to resonance enhancement of ω_{SFG} with PhO^\bullet ($C^2B_1 \leftarrow X^2B_1$ transition).⁷ Both products were directly observable. Through a global fitting procedure of the SFG response at various ω_1 wavelengths [Fig. 4(a)], the $|\chi^{(2)}|$ spectra of the independent species could be measured at the water/air interface and compared to the corresponding absorption spectra [Fig. 4(b)]. The species decaying with a 12 ps lifetime can clearly be correlated with the hydrated electron, while the species that remains at the interface with minimal decay can be correlated with PhO^\bullet .⁷

The correlation between the absorption spectrum of $e_{(\text{surf})}^-$ and $e_{(\text{aq})}^-$ strongly suggests that the electron observed at the interface is not akin to $e_{(\text{ext})}^-$ as this would be strongly red-shifted for $e_{(\text{ext})}^-$ because of its much larger size.⁸⁰ The decay lifetime of $e_{(\text{surf})}^-$ is consistent with the internalization of $e_{(\text{surf})}^-$ to $e_{(\text{aq})}^-$ based on complementary *ab initio* molecular dynamics simulations.⁷ The latter show that the electron migrates to a distance of ≥ 5 Å on a ~ 10 ps timescale, by which point the spatial distribution of $e_{(\text{aq})}^-$ (radius of gyration of $e_{(\text{aq})}^-$, $r_g = 2.35$ Å) is no longer in the non-centrosymmetric environment of the surface, and therefore no

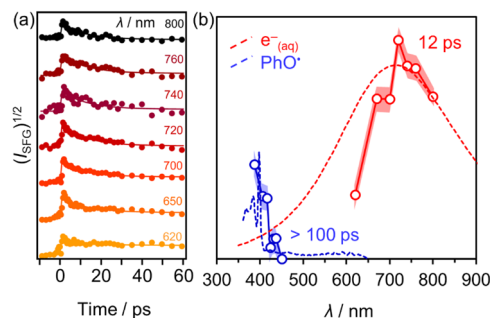


FIG. 4. (a) Kinetics of the SFG signal following photo-oxidation of the phenolate anion at the water/air interface ESFG. (b) The absorption (dotted) and ESFG response (circles) spectra of the hydrated electron (red) and the phenoxy radical (blue) and the associated lifetime of these features. Adapted with permission from Jordan *et al.*, *Nat. Commun.* **15**(1), 182 (2024). Copyright 2024 Springer Nature Limited.

longer detectable by ESFG. These results not only demonstrate the outstanding species selectivity but also the excellent surface selectivity of the TR-ESFG experiment (on the order of 3 Å).

PhO^\bullet remains at the interface as it has a surface propensity—similar to the case of the indole cation⁷³ discussed above. The electron separation from the PhO^\bullet is fundamentally different to the bulk, and geminate recombination is observed as a very minor channel. Hence, in this case, the surface acts as a driver for charge-separation, leaving a radical at the water/air interface, which may, in turn, be susceptible to chemistry from other aqueous species or atmospheric species. Indeed, a similar charge-separation has been implicated in the observation of interfacial OH^\bullet in aqueous microdroplets⁵ (which are speculated to form through field ionization of OH^- at the water/air surface¹⁰¹).

A key conclusion from TR-ESFG experiments on iodide and phenolate is that $e_{(\text{surf})}^-$ is observable by resonance-enhancement and that it appears to be quite similar to $e_{(\text{aq})}^-$ with no electronic spectral evidence that the liberated electron is akin to $e_{(\text{ext})}^-$.⁷ This is inconsistent with TR-HD-VSFG experiments, which have additionally been performed on phenol⁶—a closer comparison to phenolate—as explained next.

EXCITED STATE DYNAMICS OF PHENOL AND ENHANCED PHOTO-CHEMICAL REACTIVITY

Kusaka *et al.* applied TR-HD-VSFG to follow the dynamics of photoexcited phenol at the water/air interface.⁶ Excitation with 266 nm accesses the S_1 $1\pi\pi^*$ excited state and the products PhO^\bullet , $e_{(\text{aq})}^-$, and H_3O^+ can be expected based on bulk dynamics.¹⁰² A global fit of the time-resolved spectral evolution of the change in $\text{Im}(\chi^{(2)})$ following excitation revealed three components with spectra and lifetimes shown in Fig. 5. All three features appear within the instrument response of ~ 100 fs.⁶

The fastest component with a 300 fs decay lifetime was assigned to arising from $e_{(\text{ext})}^-$ on account of its broadly similar $\text{Im}(\chi^{(2)})$ spectrum to that observed in two-photon ionization of water and photo-oxidation of indole [Figs. 3(a) and 3(b)]. Interestingly, the slow component seen in Figs. 3(a) and 3(b) was not observed in

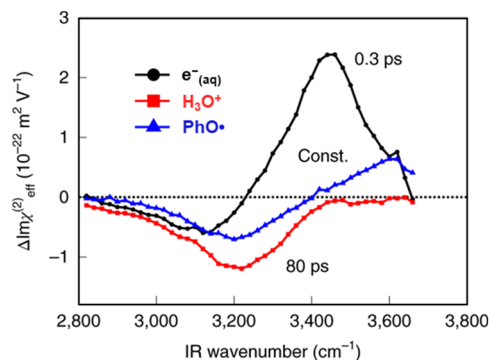


FIG. 5. Decomposed $\text{Im}(\chi^{(2)})$ spectra, showing the O–H stretching associated with the hydrated electron (black, with associated 300 fs lifetime), a hydronium cation (red, with associated 80 ps lifetime), and a phenoxy radical (blue, with a constant contribution after excitation), following excitation of phenol to the ${}^1\pi\pi^*$ state at the water/air interface. Taken with permission from Kusaka *et al.*, *Nat. Chem.* **13**(4), 306–311 (2021). Copyright 2021 Springer Nature Limited.

this experiment. Based on the $\text{Im}(\chi^{(2)})$ spectrum, the ~ 80 ps component was assigned to H_3O^+ , where the kinetics are associated with its diffusion into the bulk phase.⁹⁷ Finally, the constant offset was assigned to PhO^\bullet , which remains at the interface, in agreement with the TR-ESFG experiments probing photo-oxidation of phenolate.⁷

Comparing the observed TR-HD-VSFG dynamics to the known dynamics in the flanking phases—air (or vacuum) and water—reveals dramatically differing dynamics. In the gas-phase, excitation at 266 nm leads to H-atom loss by tunneling from the initially excited ${}^1\pi\pi^*$ state to the dissociative ${}^1\pi\sigma^*$ state (repulsive in RO-H).^{103,104} This process takes >1 ns if excited below the ${}^1\pi\pi^*/{}^1\pi\sigma^*$ conical intersection (which is the case at 266 nm).¹⁰³ In solution, the timescales are similarly slow although there is some debate about the exact mechanism leading to $e_{(\text{aq})}^-$ and H_3O^+ (autoionization from S_1 followed by deprotonation¹⁰² or charge-transfer and proton-coupled electron transfer following H-atom dissociation¹⁰⁵). Regardless, at the interface, the TR-HD-VSFG results suggest that the dynamics are accelerated by a factor of 10^4 .

The observed increase in rate has been supported by computational work¹⁰⁶ that suggests that at the water/air interface, the ${}^1\pi\pi^*/{}^1\pi\sigma^*$ conical intersection barrier is lowered so that tunneling to the ${}^1\pi\sigma^*$ state leads to a much faster rate of dissociation. In the bulk, the alcohol group of phenol forms hydrogen bonds with surrounding water molecules, which are disrupted at the interface, and this, in turn, has a stabilizing effect on the ${}^1\pi\sigma^*$ state. Much like increasing the excitation energy above the conical intersection leads to a 10^4 enhancement in the rate in both the gas and aqueous phases, simply lowering ${}^1\pi\sigma^*$ allows for 266 nm to excite above the conical intersection, leading to ultrafast dynamics. Furthermore, within a Marcus picture of charge-transfer impeded by a barrier, lowering the barrier increases the rate.¹⁰⁷ While this argument is consistent with the aqueous phase, it is not relative to the gas-phase, where there are no hydrogen bonds and a nanosecond rate is also observed. Nevertheless, there are clearly dynamics taking place on very short timescales at the interface.

Jordan *et al.* repeated the above experiment on phenol using TR-ESFG, in the same manner as for phenolate photo-oxidation,

using an ω_1 wavelength of 720 nm, resonant with the peak of $e_{(\text{surf})}^-$.¹² Remarkably, no electron signal was observed, despite being clearly sensitive to the electron (based on the phenolate work).¹² Excitation in that case was at 257 nm instead of 266 nm, but this should only increase the rates observed (as excitation is closer to the ${}^1\pi\pi^*/{}^1\pi\sigma^*$ conical intersection), so the lack of electron signal is surprising.

AN APPRAISAL OF CURRENT EVIDENCE AND SUGGESTED RESOLUTIONS

There are a number of contradictions between conclusions from TR-ESFG and TR-HD-VSFG. The former supports a picture in which the electron appears more like $e_{(\text{surf})}^-$ than $e_{(\text{ext})}^-$, while the latter concludes the opposite; while ESFG is clearly sensitive to interfacial electrons, it fails to observe these for phenol excitation (despite the larger surface concentration and similar excitation cross-section off phenol compared to phenolate), while VSFG sees a clear signature assigned to $e_{(\text{ext})}^-$. Ultimately, one should be able to develop a consistent understanding between the differing methods. We now consider some of the shortcomings of both methods.

With regards to TR-HD-VSFG, the 800 nm driving field and the 630 nm SFG field are both resonant with the absorption spectrum of $e_{(\text{aq})}^-$ [Fig. 1(a)], and as evident from the TR-ESFG experiments,⁷ this resonance-enhancement impacts the SFG signals, be they VSFG or ESFG. While resonance-enhancement with 630 nm is briefly discounted in the supporting information of the TR-HD-VSFG experiments,⁶ the consequences of the double electronic resonance condition was not. One could also question why the excited state of phenol was not considered as a possible source of differential VSFG signal. The $\text{Im}(\chi^{(2)})$ spectrum of the water interacting with the ${}^1\pi\pi^*$ state is likely to be different to that of the ground electronic state: this would have an instantaneous appearance, and subsequent internal vibrational relaxation dynamics on the ${}^1\pi\pi^*$ state is likely to be very fast. We have attempted TR-ESFG experiments aimed at probing the ${}^1\pi\pi^*$ state of phenol (through resonance-enhancement via its transient absorption spectrum¹⁰²), but this too failed to offer measurable signals.

From a broader perspective, is the OH stretch sufficiently sensitive and differential to identify specific species with which the water molecules are interacting? A positive $\text{Im}(\chi^{(2)})$ signal is associated with “free” OH bonds pointing—on average—upward [as implied schematically for $e_{(\text{ext})}^-$ in Figs. 3(a) and 3(b)]. A negative $\text{Im}(\chi^{(2)})$ signal is associated with “free” OH bonds pointing—on average—downward (which is the case in H_3O^+).^{108–111} For $e_{(\text{surf})}^-$, there may—on average—be no preferential orientation of the OH bonds around the electron at the interface, which is broadly consistent with the computational snapshot of $e_{(\text{surf})}^-$ in Fig. 1(c). Hence, the $\text{Im}(\chi^{(2)})$ spectrum probing $e_{(\text{surf})}^-$ may be very small and only weakly observable in a TR-HD-VSFG experiment. Indeed, the slower components observed in Figs. 3(a) and 3(b) are broadly consistent with the evolution of $e_{(\text{surf})}^-$ to $e_{(\text{aq})}^-$, which takes place on a 12 ps timescale for the phenolate system (probed by TR-ESFG), and their much lower intensity would be consistent with $e_{(\text{surf})}^-$, producing a weaker $\text{Im}(\chi^{(2)})$ signal. The weak $\text{Im}(\chi^{(2)})$ response might also explain why no slow component was observed in the experiments on phenol. Taken together, this then leads to the interesting

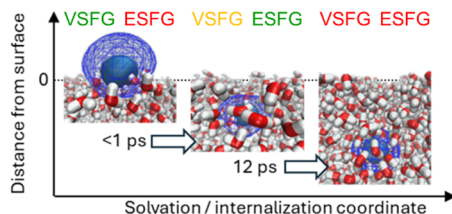


FIG. 6. Schematic showing the suggested sensitivity of vibrational and electronic SFG to differing electronic distributions of the electron relative to the water/air dividing surface. Green indicates a signal is observable, orange is weakly observable, and red is not observable. Snapshots taken with permission from Jordan *et al.*, Nat. Commun. **15**(1), 182 (2024). Copyright 2024 Springer Nature Limited.

possibility that the TR-HD-VSFG is predominantly sensitive to $e^-_{(ext)}$ and less so to $e^-_{(surf)}$, which would be broadly consistent with the very short decay times observed in the TR-HD-VSFG experiments (ranging from 300 fs⁶ to 1.2 ps⁷³ for the fast components) that agree with simulations of the decay of a very diffuse electron at the surface.⁸⁷ In contrast, the TR-ESFG experiments then appear to only be sensitive to $e^-_{(surf)}$ and not to $e^-_{(ext)}$. We do not know why we should not be sensitive to $e^-_{(ext)}$ because the driving fields would still lead to some resonance enhancement (even if the absorption spectrum is red-shifted) and the hyperpolarizability is expected to be very large.¹¹² Nevertheless, it would explain why the TR-ESFG experiments only observe a longer decay lifetime of 12 ps⁷, which is again consistent with the simulations.⁸⁷ These conclusions are summarized in Fig. 6. Note that in the first surface experiments probing $e^-_{(surf)}$ using TR-ESHG, a very large signal was observed (which arose from 2-photon excitation) that decayed on a sub-ps timescale, which could be consistent with $e^-_{(ext)}$.⁷² As to why no electrons are observed in the TR-ESFG experiments on phenol, perhaps the dynamics of $e^-_{(surf)}$ from phenol are too fast to be captured with the time-resolution of ~ 200 fs and excitation at 257 nm, which is expected to lead to even faster dynamics than observed in the TR-HD-VSFG experiments.

There are further puzzling questions. The $\text{Im}(\chi^{(2)})$ spectra obtained for the interfacial electrons broadly follow the IR spectrum of the small water cluster anion,^{61,76} but are these small clusters suitable proxies for what $e^-_{(ext)}$ might look like in the bulk?⁷⁴ On the other hand, for the TR-ESFG experiments, the absorption spectrum of $e^-_{(aq)}$ is very broad and contains several transitions, which may not be faithfully captured by the homodyne-detected ESFG experiments.

The comparison between phenolate and phenol is not ideal, and the pump wavelengths of the two experiments differ. This is where we hope we can inspire a series of new experiments. It would be of interest to see results from TR-HD-VSFG experiments following photo-oxidation of phenolate. Unfortunately, at 266 nm, in the bulk at least, dynamics are significantly slower,¹⁰⁰ so this may not aid the comparison unless they can be done at the same pump wavelength of 257 nm as in the TR-ESFG experiments. With regards to phenol, it would certainly be interesting to perform TR-ESFG experiments at shorter ω_1 wavelengths than the wavelength used to date (720 nm), which was not resonant with PhO^\bullet ; being able to observe the formation of PhO^\bullet following excitation of the $^1\pi\pi^*$ state in phenol would offer a direct comparable measure to the TR-HD-VSFG

experiment, even if excited at a different wavelength. These experiments are currently underway. Finally, it would be interesting to develop and perform TR-HD-ESFG.

CONCLUSION

We have summarized a comparison between recent results from time-resolved electronic and vibrational sum-frequency generation spectroscopy forming hydrated electrons at the aqueous/air interface. While both methods indicate that electrons are observable, the conclusions drawn from those experiments in terms of the nature of the electron (whether it is external to water with most of its electron density in the vapor phase or it appears more like a hydrated electron at the interface with most of its electron density in the aqueous phase) and the kinetics of its solvation and internalization differ. Developing a consistent view across different methods is clearly very important as the conclusions drawn from experiments may have significant consequences on—for example—atmospheric chemistry. To the best of our knowledge, there are no TR-ESFG and TR-VSFG experiments that are directly comparable to offer this consistent view. Instead, we offer a series of suggestions for future experiments that might resolve discrepancies in the interpretation of photodynamics, and we suggest that phenol and/or phenolate are useful test systems from this perspective. More broadly, we hope to have highlighted the caution that should be taken when interpreting data from a single set of spectroscopic measurements. In the same vein as bulk studies commonly using transient electronic and vibrational absorption spectroscopy, it would be beneficial for complementary methods to be deployed for specific interfacial processes.

ACKNOWLEDGMENTS

This work was supported by the Engineering and Physical Sciences Research Council (Grant No. EP/R513039/1) and the Leverhulme Trust Grant No. RPG-2023-043.

AUTHOR DECLARATIONS

Conflict of Interest

The authors have no conflicts to disclose.

Author Contributions

Faith G. Pritchard: Writing – original draft (equal); Writing – review & editing (equal). **Caleb J. C. Jordan:** Writing – original draft (supporting); Writing – review & editing (equal). **Jan R. R. Verlet:** Writing – original draft (equal); Writing – review & editing (equal).

DATA AVAILABILITY

Data sharing is not applicable to this article as no new data were created or analyzed in this study.

REFERENCES

- Y. Jung and R. A. Marcus, “On the theory of organic catalysis ‘on water,’” *J. Am. Chem. Soc.* **129**(17), 5492–5502 (2007).
- A. Chanda and V. V. Fokin, “Organic synthesis ‘on water,’” *Chem. Rev.* **109**(2), 725–748 (2009).

- ³X. Yan, R. M. Bain, and R. G. Cooks, "Organic reactions in microdroplets: Reaction acceleration revealed by mass spectrometry," *Angew. Chem., Int. Ed.* **55**(42), 12960–12972 (2016).
- ⁴S. Banerjee, E. Gnanamani, X. Yan, and R. N. Zare, "Can all bulk-phase reactions be accelerated in microdroplets?," *Analyst* **142**(9), 1399–1402 (2017).
- ⁵J. K. Lee, D. Samanta, H. G. Nam, and R. N. Zare, "Micrometer-sized water droplets induce spontaneous reduction," *J. Am. Chem. Soc.* **141**(27), 10585–10589 (2019).
- ⁶R. Kusaka, S. Nihonyanagi, and T. Tahara, "The photochemical reaction of phenol becomes ultrafast at the air–water interface," *Nat. Chem.* **13**(4), 306–311 (2021).
- ⁷C. J. C. Jordan, M. P. Coons, J. M. Herbert, and J. R. R. Verlet, "Spectroscopy and dynamics of the hydrated electron at the water/air interface," *Nat. Commun.* **15**(1), 182 (2024).
- ⁸F. Perakis, L. De Marco, A. Shalit, F. Tang, Z. R. Kann, T. D. Kühne, R. Torre, M. Bonn, and Y. Nagata, "Vibrational spectroscopy and dynamics of water," *Chem. Rev.* **116**(13), 7590–7607 (2016).
- ⁹M. F. Ruiz-Lopez, J. S. Francisco, M. T. C. Martins-Costa, and J. M. Anglada, "Molecular reactions at aqueous interfaces," *Nat. Rev. Chem.* **4**(9), 459–475 (2020).
- ¹⁰S. Rossignol, L. Tinel, A. Bianco, M. Passananti, M. Brigante, D. J. Donaldson, and C. George, "Atmospheric photochemistry at a fatty acid-coated air–water interface," *Science* **353**(6300), 699–702 (2016).
- ¹¹K. J. Kappes, A. M. Deal, M. F. Jepsen, S. L. Blair, J.-F. Doussin, M. Cazaunau, E. Pangui, B. N. Hopper, M. S. Johnson, and V. Vaida, "Chemistry and photochemistry of pyruvic acid at the air–water interface," *J. Phys. Chem. A* **125**(4), 1036–1049 (2021).
- ¹²C. J. C. Jordan, E. A. Lowe, and J. R. R. Verlet, "Photooxidation of the phenolate anion is accelerated at the water/air interface," *J. Am. Chem. Soc.* **144**(31), 14012–14015 (2022).
- ¹³S. R. Mercier, O. V. Boyarkin, A. Kamariotis, M. Guglielmi, I. Tavernelli, M. Casella, U. Rothlisberger, and T. R. Rizzo, "Microsolvation effects on the excited-state dynamics of protonated tryptophan," *J. Am. Chem. Soc.* **128**(51), 16938–16943 (2006).
- ¹⁴W. Zagorec-Marks, M. M. Foreman, J. R. R. Verlet, and J. M. Weber, "Probing the microsolvation environment of the green fluorescent protein chromophore *in vacuo*," *J. Phys. Chem. Lett.* **11**(5), 1940–1946 (2020).
- ¹⁵T. F. Heinz, C. K. Chen, D. Ricard, and Y. R. Shen, "Spectroscopy of molecular monolayers by resonant second-harmonic generation," *Phys. Rev. Lett.* **48**(7), 478–481 (1982).
- ¹⁶Y. R. Shen, "Surface properties probed by second-harmonic and sum-frequency generation," *Nature* **337**(6207), 519–525 (1989).
- ¹⁷R. Superfine, J. Y. Huang, and Y. R. Shen, "Phase measurement for surface infrared–visible sum-frequency generation," *Opt. Lett.* **15**(22), 1276–1278 (1990).
- ¹⁸K. B. Eisenthal, "Liquid interfaces probed by second-harmonic and sum-frequency spectroscopy," *Chem. Rev.* **96**, 1343–1360 (1996).
- ¹⁹G. L. Richmond, "Molecular bonding and interactions at aqueous surfaces as probed by vibrational sum frequency spectroscopy," *Chem. Rev.* **102**(8), 2693–2724 (2002).
- ²⁰Y. R. Shen and V. Ostroverkhov, "Sum-frequency vibrational spectroscopy on water interfaces: Polar orientation of water molecules at interfaces," *Chem. Rev.* **106**(4), 1140–1154 (2006).
- ²¹A. M. Jubb, W. Hua, and H. C. Allen, "Environmental chemistry at vapor/water interfaces: Insights from vibrational sum frequency generation spectroscopy," *Annu. Rev. Phys. Chem.* **63**(1), 107–130 (2012).
- ²²M. Bonn, Y. Nagata, and E. H. G. Backus, "Molecular structure and dynamics of water at the water–air interface studied with surface-specific vibrational spectroscopy," *Angew. Chem., Int. Ed.* **54**(19), 5560–5576 (2015).
- ²³S. Yamaguchi and T. Otsu, "Progress in phase-sensitive sum frequency generation spectroscopy," *Phys. Chem. Chem. Phys.* **23**(34), 18253–18267 (2021).
- ²⁴Y.-R. Shen, *The Principles of Nonlinear Optics* (Wiley, 2002).
- ²⁵Y. R. Shen, "Phase-sensitive sum-frequency spectroscopy," *Annu. Rev. Phys. Chem.* **64**(1), 129–150 (2013).
- ²⁶I. V. Stiopkin, H. D. Jayatilake, A. N. Bordenyuk, and A. V. Benderskii, "Heterodyne-detected vibrational sum frequency generation spectroscopy," *J. Am. Chem. Soc.* **130**(7), 2271–2275 (2008).
- ²⁷W. Xiong, J. E. Laaser, R. D. Mehlenbacher, and M. T. Zanni, "Adding a dimension to the infrared spectra of interfaces using heterodyne detected 2D sum-frequency generation (HD 2D SFG) spectroscopy," *Proc. Natl. Acad. Sci. U. S. A.* **108**(52), 20902–20907 (2011).
- ²⁸S. Nihonyanagi, J. A. Mondal, S. Yamaguchi, and T. Tahara, "Structure and dynamics of interfacial water studied by heterodyne-detected vibrational sum-frequency generation," *Annu. Rev. Phys. Chem.* **64**(1), 579–603 (2013).
- ²⁹M. D. Boamah, P. E. Ohno, E. Lozier, J. Van Ardenne, and F. M. Geiger, "Specific about specific ion adsorption from heterodyne-detected second harmonic generation," *J. Phys. Chem. B* **123**(27), 5848–5856 (2019).
- ³⁰K. Inoue, M. Ahmed, S. Nihonyanagi, and T. Tahara, "Reorientation-induced relaxation of free OH at the air/water interface revealed by ultrafast heterodyne-detected nonlinear spectroscopy," *Nat. Commun.* **11**(1), 5344 (2020).
- ³¹S. Yamaguchi and T. Tahara, "Heterodyne-detected electronic sum frequency generation: 'Up' versus 'down' alignment of interfacial molecules," *J. Chem. Phys.* **129**(10), 101102 (2008).
- ³²F. Tang, T. Ohto, S. Sun, J. R. Rouxel, S. Imoto, E. H. G. Backus, S. Mukamel, M. Bonn, and Y. Nagata, "Molecular structure and modeling of water–air and ice–air interfaces monitored by sum-frequency generation," *Chem. Rev.* **120**(8), 3633–3667 (2020).
- ³³Y. Litman, K.-Y. Chiang, T. Seki, Y. Nagata, and M. Bonn, "Surface stratification determines the interfacial water structure of simple electrolyte solutions," *Nat. Chem.* **16**(4), 644–650 (2024).
- ³⁴K.-Y. Chiang, T. Seki, C.-C. Yu, T. Ohto, J. Hunger, M. Bonn, and Y. Nagata, "The dielectric function profile across the water interface through surface-specific vibrational spectroscopy and simulations," *Proc. Natl. Acad. Sci. U. S. A.* **119**(36), e2204156119 (2022).
- ³⁵S. T. van der Post, C.-S. Hsieh, M. Okuno, Y. Nagata, H. J. Bakker, M. Bonn, and J. Hunger, "Strong frequency dependence of vibrational relaxation in bulk and surface water reveals sub-picosecond structural heterogeneity," *Nat. Commun.* **6**(1), 8384 (2015).
- ³⁶X. Shi, E. Borguet, A. N. Tarnovsky, and K. B. Eisenthal, "Ultrafast dynamics and structure at aqueous interfaces by second harmonic generation," *Chem. Phys.* **205**(1–2), 167–178 (1996).
- ³⁷E. V. Sitzmann and K. B. Eisenthal, "Dynamics of intermolecular electronic energy transfer at an air/liquid interface," *J. Chem. Phys.* **90**(5), 2831–2832 (1989).
- ³⁸A. Castro, E. V. Sitzmann, D. Zhang, and K. B. Eisenthal, "Rotational relaxation at the air/water interface by time-resolved second harmonic generation," *J. Phys. Chem.* **95**(18), 6752–6753 (1991).
- ³⁹K. Sekiguchi, S. Yamaguchi, and T. Tahara, "Femtosecond time-resolved electronic sum-frequency generation spectroscopy: A new method to investigate ultrafast dynamics at liquid interfaces," *J. Chem. Phys.* **128**(11), 114715 (2008).
- ⁴⁰A. Punzi, G. Martin-Gassin, J. Grilj, and E. Vauthey, "Effect of salt on the excited-state dynamics of malachite green in bulk aqueous solutions and at air/water interfaces: A femtosecond transient absorption and surface second harmonic generation study," *J. Phys. Chem. C* **113**(27), 11822–11829 (2009).
- ⁴¹P. Sen, S. Yamaguchi, and T. Tahara, "Ultrafast dynamics of malachite green at the air/water interface studied by femtosecond time-resolved electronic sum frequency generation (TR-ESFG): An indicator for local viscosity," *Faraday Discuss.* **145**, 411–428 (2010).
- ⁴²L. Foglia, M. Wolf, and J. Stähler, "Ultrafast dynamics in solids probed by femtosecond time-resolved broadband electronic sum frequency generation," *Appl. Phys. Lett.* **109**(20), 202106 (2016).
- ⁴³S. Richert, M. Fedoseeva, and E. Vauthey, "Ultrafast photoinduced dynamics at air/liquid and liquid/liquid interfaces," *J. Phys. Chem. Lett.* **3**(12), 1635–1642 (2012).
- ⁴⁴M. Fedoseeva, R. Letrun, and E. Vauthey, "Excited-state dynamics of rhodamine 6G in aqueous solution and at the dodecane/water interface," *J. Phys. Chem. B* **118**(19), 5184–5193 (2014).
- ⁴⁵S. Richert, S. Mosquera Vazquez, M. Grzybowski, D. T. Gryko, A. Kyrychenko, and E. Vauthey, "Excited-state dynamics of an environment-sensitive push–pull diketopyrrolopyrrole: Major differences between the bulk solution phase and the dodecane/water interface," *J. Phys. Chem. B* **118**(33), 9952–9963 (2014).
- ⁴⁶G.-H. Deng, Y. Qian, T. Zhang, J. Han, H. Chen, and Y. Rao, "Two-dimensional electronic–vibrational sum frequency spectroscopy for interactions of electronic

- and nuclear motions at interfaces," *Proc. Natl. Acad. Sci. U. S. A.* **118**(34), e2100608118 (2021).
- ⁴⁷G.-H. Deng, Y. Qian, and Y. Rao, "Development of ultrafast broadband electronic sum frequency generation for charge dynamics at surfaces and interfaces," *J. Chem. Phys.* **150**(2), 024708 (2019).
- ⁴⁸I. V. Stiopkin, C. Weeraman, P. A. Pieniazek, F. Y. Shalhout, J. L. Skinner, and A. V. Benderskii, "Hydrogen bonding at the water surface revealed by isotopic dilution spectroscopy," *Nature* **474**(7350), 192–195 (2011).
- ⁴⁹D. Ojha, N. K. Kaliannan, and T. D. Kühne, "Time-dependent vibrational sum-frequency generation spectroscopy of the air-water interface," *Commun. Chem.* **2**(1), 116 (2019).
- ⁵⁰W. Sung, K. Inoue, S. Nihonyanagi, and T. Tahara, "Unified picture of vibrational relaxation of OH stretch at the air/water interface," *Nat. Commun.* **15**(1), 1258 (2024).
- ⁵¹E. J. Hart and J. W. Boag, "Absorption spectrum of the hydrated electron in water and in aqueous solutions," *J. Am. Chem. Soc.* **84**(21), 4090–4095 (1962).
- ⁵²J. M. Herbert and M. P. Coons, "The hydrated electron," *Annu. Rev. Phys. Chem.* **68**(1), 447–472 (2017).
- ⁵³A. M. Rizzuto, S. Irgen-Giuro, A. Eftekhari-Bafrooei, and R. J. Saykally, "Broadband deep UV spectra of interfacial aqueous iodide," *J. Phys. Chem. Lett.* **7**(19), 3882–3885 (2016).
- ⁵⁴S. Yamaguchi and T. Tahara, "Development of electronic sum frequency generation spectroscopies and their application to liquid interfaces," *J. Phys. Chem. C* **119**(27), 14815–14828 (2015).
- ⁵⁵C. J. C. Jordan and J. R. R. Verlet, "Time-resolved electronic sum-frequency generation spectroscopy with fluorescence suppression using optical Kerr gating," *J. Chem. Phys.* **155**(16), 164202 (2021).
- ⁵⁶B. C. Garrett, D. A. Dixon, D. M. Camaioni, D. M. Chipman, M. A. Johnson, C. D. Jonah, G. A. Kimmel, J. H. Miller, T. N. Rescigno, P. J. Rosicky, S. S. Xantheas, S. D. Colson, A. H. Laufer, D. Ray, P. F. Barbara, D. M. Bartels, K. H. Becker, K. H. Bowen, Jr., S. E. Bradforth, I. Carmichael, J. V. Coe, L. R. Corrales, J. P. Cowin, M. Dupuis, K. B. Eisenthal, J. A. Franz, M. S. Gutowski, K. D. Jordan, B. D. Kay, J. A. LaVerne, S. V. Lymar, T. E. Madey, C. W. McCurdy, D. Meisel, S. Mukamel, A. R. Nilsson, T. M. Orlando, N. G. Petrik, S. M. Pimblott, J. R. Rustad, G. K. Schenter, S. J. Singer, A. Tokmakoff, L.-S. Wang, and T. S. Zwier, "Role of water in electron-initiated processes and radical chemistry: Issues and scientific advances," *Chem. Rev.* **105**(1), 355–390 (2005).
- ⁵⁷E. Alizadeh and L. Sanche, "Precursors of solvated electrons in radiobiological physics and chemistry," *Chem. Rev.* **112**(11), 5578–5602 (2012).
- ⁵⁸L. D. Jacobson and J. M. Herbert, "Polarization-bound quasi-continuum states are responsible for the 'blue tail' in the optical absorption spectrum of the aqueous electron," *J. Am. Chem. Soc.* **132**(29), 10000–10002 (2010).
- ⁵⁹L. D. Jacobson and J. M. Herbert, "Theoretical characterization of four distinct isomer types in hydrated-electron clusters, and proposed assignments for photoelectron spectra of water cluster anions," *J. Am. Chem. Soc.* **133**(49), 19889–19899 (2011).
- ⁶⁰P. J. Low, W. Chu, Z. Nie, M. S. Bin Mohd Yusof, O. V. Prezhdo, and Z.-H. Loh, "Observation of a transient intermediate in the ultrafast relaxation dynamics of the excess electron in strong-field-ionized liquid water," *Nat. Commun.* **13**(1), 7300 (2022).
- ⁶¹N. I. Hammer, J. R. Roscioli, J. C. Bopp, J. M. Headrick, and M. A. Johnson, "Vibrational predissociation spectroscopy of the $(\text{H}_2\text{O})_{6-21}^-$ clusters in the OH stretching region: Evolution of the excess electron-binding signature into the intermediate cluster size regime," *J. Chem. Phys.* **123**(24), 244311 (2005).
- ⁶²L. Kevan, "Solvated electron structure in glassy matrixes," *Acc. Chem. Res.* **14**(5), 138–145 (1981).
- ⁶³R. E. Larsen, W. J. Glover, and B. J. Schwartz, "Does the hydrated electron occupy a cavity?," *Science* **329**(5987), 65–69 (2010).
- ⁶⁴J. Savolainen, F. Uhlig, S. Ahmed, P. Hamm, and P. Jungwirth, "Direct observation of the collapse of the delocalized excess electron in water," *Nat. Chem.* **6**(8), 697–701 (2014).
- ⁶⁵A. Kumar, J. A. Walker, D. M. Bartels, and M. D. Sevilla, "A simple *ab initio* model for the hydrated electron that matches experiment," *J. Phys. Chem. A* **119**(34), 9148–9159 (2015).
- ⁶⁶O. Marsalek, F. Uhlig, J. VandeVondele, and P. Jungwirth, "Structure, dynamics, and reactivity of hydrated electrons by *ab initio* molecular dynamics," *Acc. Chem. Res.* **45**(1), 23–32 (2012).
- ⁶⁷C. Silva, P. K. Walhout, K. Yokoyama, and P. F. Barbara, "Femtosecond solvation dynamics of the hydrated electron," *Phys. Rev. Lett.* **80**(5), 1086–1089 (1998).
- ⁶⁸A. E. Bragg, J. R. R. Verlet, A. Kammrath, O. Cheshnovsky, and D. M. Neumark, "Hydrated electron dynamics: From clusters to bulk," *Science* **306**(5696), 669–671 (2004).
- ⁶⁹M. H. Elkins, H. L. Williams, A. T. Shreve, and D. M. Neumark, "Relaxation mechanism of the hydrated electron," *Science* **342**(6165), 1496–1499 (2013).
- ⁷⁰K. R. Siefermann, Y. Liu, E. Lugovoy, O. Link, M. Faubel, U. Buck, B. Winter, and B. Abel, "Binding energies, lifetimes and implications of bulk and interface solvated electrons in water," *Nat. Chem.* **2**(4), 274–279 (2010).
- ⁷¹A. Lübcke, F. Buchner, N. Heine, I. V. Hertel, and T. Schultz, "Time-resolved photoelectron spectroscopy of solvated electrons in aqueous NaI solution," *Phys. Chem. Chem. Phys.* **12**(43), 14629–14634 (2010).
- ⁷²D. M. Sagar, C. D. Bain, and J. R. R. Verlet, "Hydrated electrons at the water/air interface," *J. Am. Chem. Soc.* **132**(20), 6917–6919 (2010).
- ⁷³K. Matsuzaki, R. Kusaka, S. Nihonyanagi, S. Yamaguchi, T. Nagata, and T. Tahara, "Partially hydrated electrons at the air/water interface observed by UV-excited time-resolved heterodyne-detected vibrational sum frequency generation spectroscopy," *J. Am. Chem. Soc.* **138**(24), 7551–7557 (2016).
- ⁷⁴J. V. Coe, "Fundamental properties of bulk water from cluster ion data," *Int. Rev. Phys. Chem.* **20**(1), 33–58 (2001).
- ⁷⁵J. V. Coe, G. H. Lee, J. G. Eaton, S. T. Arnold, H. W. Sarkas, K. H. Bowen, C. Ludewigt, H. Haberland, and D. R. Worsnop, "Photoelectron spectroscopy of hydrated electron cluster anions, $(\text{H}_2\text{O})_{n=2-69}^-$," *J. Chem. Phys.* **92**(6), 3980–3982 (1990).
- ⁷⁶N. I. Hammer, J.-W. Shin, J. M. Headrick, E. G. Diken, J. R. Roscioli, G. H. Weddle, and M. A. Johnson, "How do small water clusters bind an excess electron?," *Science* **306**(5696), 675–679 (2004).
- ⁷⁷J. R. R. Verlet, A. E. Bragg, A. Kammrath, O. Cheshnovsky, and D. M. Neumark, "Observation of large water-cluster anions with surface-bound excess electrons," *Science* **307**(5706), 93–96 (2005).
- ⁷⁸N. I. Hammer, J. R. Roscioli, and M. A. Johnson, "Identification of two distinct electron binding motifs in the anionic water clusters: A vibrational spectroscopic study of the $(\text{H}_2\text{O})_6^-$ isomers," *J. Phys. Chem. A* **109**(35), 7896–7901 (2005).
- ⁷⁹J. R. Roscioli, N. I. Hammer, and M. A. Johnson, "Infrared spectroscopy of water cluster anions, $(\text{H}_2\text{O})_{n=3-24}^-$ in the HOH bending region: Persistence of the double H-bond acceptor (AA) water molecule in the excess electron binding site of the class I isomers," *ChemInform* **37**(35), 7517–7520 (2006).
- ⁸⁰P. Ayotte and M. A. Johnson, "Electronic absorption spectra of size-selected hydrated electron clusters: $(\text{H}_2\text{O})_n^-$, $n = 6-50$," *J. Chem. Phys.* **106**(2), 811–814 (1997).
- ⁸¹A. Herburger, E. Barwa, M. Ončák, J. Heller, C. van der Linde, D. M. Neumark, and M. K. Beyer, "Probing the structural evolution of the hydrated electron in water cluster anions $(\text{H}_2\text{O})_n^-$, $n \leq 200$, by electronic absorption spectroscopy," *J. Am. Chem. Soc.* **141**(45), 18000–18003 (2019).
- ⁸²J. R. Roscioli and M. A. Johnson, "Isomer-specific spectroscopy of the $(\text{H}_2\text{O})_8^-$ cluster anion in the intramolecular bending region by selective photodepletion of the more weakly electron binding species (isomer II)," *J. Chem. Phys.* **126**(2), 024307 (2007).
- ⁸³L. Ma, K. Majer, F. Chirof, and B. von Issendorff, "Low temperature photoelectron spectra of water cluster anions," *J. Chem. Phys.* **131**(14), 144303 (2009).
- ⁸⁴A. Lietard and J. R. R. Verlet, "Selectivity in electron attachment to water clusters," *J. Phys. Chem. Lett.* **10**(6), 1180–1184 (2019).
- ⁸⁵B. Abel, "Hydrated interfacial ions and electrons," *Annu. Rev. Phys. Chem.* **64**(1), 533–552 (2013).
- ⁸⁶P. Jungwirth and D. J. Tobias, "Ions at the air/water interface," *J. Phys. Chem. B* **106**(25), 6361–6373 (2002).
- ⁸⁷M. P. Coons, Z.-Q. You, and J. M. Herbert, "The hydrated electron at the surface of neat liquid water appears to be indistinguishable from the bulk species," *J. Am. Chem. Soc.* **138**(34), 10879–10886 (2016).

- ⁸⁸F. Buchner, T. Schultz, and A. Lübcke, "Solvated electrons at the water–air interface: Surface versus bulk signal in low kinetic energy photoelectron spectroscopy," *Phys. Chem. Chem. Phys.* **14**(16), 5837–5842 (2012).
- ⁸⁹J. R. R. Verlet, A. Kamrath, G. B. Griffin, and D. M. Neumark, "Electron solvation in water clusters following charge transfer from iodide," *J. Chem. Phys.* **123**(23), 231102 (2005).
- ⁹⁰P. J. Nowakowski, D. A. Woods, and J. R. R. Verlet, "Charge transfer to solvent dynamics at the ambient water/air interface," *J. Phys. Chem. Lett.* **7**(20), 4079–4085 (2016).
- ⁹¹J. A. Kloepfer, V. H. Vilchiz, V. A. Lenchenkov, A. C. Germaine, and S. E. Bradforth, "The ejection distribution of solvated electrons generated by the one-photon photodetachment of aqueous I^- and two-photon ionization of the solvent," *J. Chem. Phys.* **113**(15), 6288–6307 (2000).
- ⁹²V. H. Vilchiz, J. A. Kloepfer, A. C. Germaine, V. A. Lenchenkov, and S. E. Bradforth, "Map for the relaxation dynamics of hot photoelectrons injected into liquid water via anion threshold photodetachment and above threshold solvent ionization," *J. Phys. Chem. A* **105**(10), 1711–1723 (2001).
- ⁹³X. Chen and S. E. Bradforth, "The ultrafast dynamics of photodetachment," *Annu. Rev. Phys. Chem.* **59**(1), 203–231 (2008).
- ⁹⁴P. J. Nowakowski, D. A. Woods, C. D. Bain, and J. R. R. Verlet, "Time-resolved phase-sensitive second harmonic generation spectroscopy," *J. Chem. Phys.* **142**(8), 084201 (2015).
- ⁹⁵F. Messina, O. Bräm, A. Cannizzo, and M. Chergui, "Real-time observation of the charge transfer to solvent dynamics," *Nat. Commun.* **4**(1), 2119–2126 (2013).
- ⁹⁶R. N. Barnett, R. Giniger, O. Cheshnovsky, and U. Landman, "Dielectron attachment and hydrogen evolution reaction in water clusters," *J. Phys. Chem. A* **115**(25), 7378–7391 (2011).
- ⁹⁷C. Tian, N. Ji, G. A. Waychunas, and Y. R. Shen, "Interfacial structures of acidic and basic aqueous solutions," *J. Am. Chem. Soc.* **130**(39), 13033–13039 (2008).
- ⁹⁸X. Chen, D. S. Larsen, S. E. Bradforth, and I. H. M. van Stokkum, "Broadband spectral probing revealing ultrafast photochemical branching after ultraviolet excitation of the aqueous phenolate anion," *J. Phys. Chem. A* **115**(16), 3807–3819 (2011).
- ⁹⁹A. L. Tyson and J. R. R. Verlet, "On the mechanism of phenolate photo-oxidation in aqueous solution," *J. Phys. Chem. B* **123**(10), 2373–2379 (2019).
- ¹⁰⁰K. Robertson, W. G. Fortune, J. A. Davies, A. N. Boichenko, M. S. Scholz, O. Tau, A. V. Bochenkova, and H. H. Fielding, "Wavelength dependent mechanism of phenolate photooxidation in aqueous solution," *Chem. Sci.* **14**(12), 3257–3264 (2023).
- ¹⁰¹J. P. Heindel, H. Hao, R. A. LaCour, and T. Head-Gordon, "Spontaneous Formation of hydrogen peroxide in water microdroplets," *J. Phys. Chem. Lett.* **13**(43), 10035–10041 (2022).
- ¹⁰²T. A. A. Oliver, Y. Zhang, A. Roy, M. N. R. Ashfold, and S. E. Bradforth, "Exploring autoionization and photoinduced proton-coupled electron transfer pathways of phenol in aqueous solution," *J. Phys. Chem. Lett.* **6**(20), 4159–4164 (2015).
- ¹⁰³G. M. Roberts, A. S. Chatterley, J. D. Young, and V. G. Stavros, "Direct observation of hydrogen tunneling dynamics in photoexcited phenol," *J. Phys. Chem. Lett.* **3**(3), 348–352 (2012).
- ¹⁰⁴G. M. Roberts and V. G. Stavros, "The role of $\pi\sigma^*$ states in the photochemistry of heteroaromatic biomolecules and their subunits: Insights from gas-phase femtosecond spectroscopy," *Chem. Sci.* **5**(5), 1698–1722 (2014).
- ¹⁰⁵J. W. Riley, B. Wang, J. L. Woodhouse, M. Assmann, G. A. Worth, and H. H. Fielding, "Unravelling the role of an aqueous environment on the electronic structure and ionization of phenol using photoelectron spectroscopy," *J. Phys. Chem. Lett.* **9**(4), 678–682 (2018).
- ¹⁰⁶T. Ishiyama, T. Tahara, and A. Morita, "Why the photochemical reaction of phenol becomes ultrafast at the air–water interface: The effect of surface hydration," *J. Am. Chem. Soc.* **144**(14), 6321–6325 (2022).
- ¹⁰⁷R. A. Marcus, "Chemical and electrochemical electron-transfer theory," *Annu. Rev. Phys. Chem.* **15**(1), 155–196 (1964).
- ¹⁰⁸Q. Du, R. Superfine, E. Freysz, and Y. R. Shen, "Vibrational spectroscopy of water at the vapor/water interface," *Phys. Rev. Lett.* **70**(15), 2313–2316 (1993).
- ¹⁰⁹N. Ji, V. Ostroverkhov, C. S. Tian, and Y. R. Shen, "Characterization of vibrational resonances of water–vapor interfaces by phase-sensitive sum-frequency spectroscopy," *Phys. Rev. Lett.* **100**(9), 096102 (2008).
- ¹¹⁰S. Nihonyanagi, S. Yamaguchi, and T. Tahara, "Direct evidence for orientational flip-flop of water molecules at charged interfaces: A heterodyne-detected vibrational sum frequency generation study," *J. Chem. Phys.* **130**(20), 204704 (2009).
- ¹¹¹S. Nihonyanagi, R. Kusaka, K. Inoue, A. Adhikari, S. Yamaguchi, and T. Tahara, "Accurate determination of complex $\chi^{(2)}$ spectrum of the air/water interface," *J. Chem. Phys.* **143**(12), 124707 (2015).
- ¹¹²W. Chen, Z.-R. Li, D. Wu, F.-L. Gu, X.-Y. Hao, B.-Q. Wang, R.-J. Li, and C.-C. Sun, "The static polarizability and first hyperpolarizability of the water trimer anion: *Ab initio* study," *J. Chem. Phys.* **121**(21), 10489–10494 (2004).